

# Analysis of the Structural Response of a 2919 GT Ro-Ro Ship Due to Changes in Hull Construction Length

Imam Pujo Mulyanto<sup>1</sup>, Ahmad Fauzan Zakki<sup>2</sup>, Kuku Prakoso Wicaksono<sup>3</sup>, Berlian Arswendo Adietya<sup>4\*</sup>  
Tuswan<sup>5</sup>

(Received: 30 October 2024 / Revised: 26 November 2024 / Accepted: 07 December 2024 / Available  
Online: 31 December 2024)

**Abstract** — On the 2919 GT Ro-Ro vessel, structural geometry changes, specifically in the Length Between Perpendiculars (LPP) with additional framing, lead to variations in loading and maximum stress, in accordance with Biro Klasifikasi Indonesia (BKI) regulations in Volume II. Finite Element Method analysis reveals structural responses, particularly in the parallel middle body section. Initially, the vessel was 10.5 meters long to support loads of seven 20-foot trucks; modifications increased this to 13.5 meters for loads of seven 40-foot trucks and 18 meters for a combination of 20-foot and 40-foot truck loads. The analysis results indicate significant differences in the vessel's maximum structural stress under truck-loaded conditions. For lengths of 10.5 meters, 13.5 meters, and 18 meters, the stresses remain within safe limits under all conditions (Calm Water, Sagging, and Hogging), with  $\sigma_{ult}$  lower than the allowable as set by BKI. However, the 18-meter length exhibits maximum stress approaching the safe threshold in the Hogging condition, with  $\sigma_{ult}$  = reaching 243.4 MPa, suggesting structural modifications are required to ensure vessel safety.

**Keywords**— Structure Geometry, Stress, Finite Element Method, Parallel Middle Body.

## I. INTRODUCTION

Designing is a crucial initial step in creating a product, including shipbuilding. In this context, designing the ship's construction system becomes a key priority before proceeding to the building phase. The steel structure of a ship plays a fundamental role in supporting its shape and construction. An essential principle in structural design is ensuring compliance with standard regulations, measured through the structure's ability to withstand loads according to applicable classification rules. One method for studying ship structures is by using the nonlinear finite element method, aimed at analyzing the estimated structural response of the ship.

Structural strength is one of the key aspects that influences the safety level of a vessel. Mubarak's research has also analyzed the ship's structural construction when subjected to static loads, which can lead to issues such as deformation and cracking. Meanwhile, continuous dynamic loads can result in fatigue. Therefore, the ship's

structural construction must maintain stress within the allowable limits, ensuring it is acceptable for the structure and possesses sufficient elastic stiffness [1].

Several studies have proposed efficient analyses for assessing the structural strength of ship constructions under monotonic bending loads using global nonlinear finite element methods. Tekgoz et al. analyzed the effects of structural damage and residual load-carrying capacity on container ships subjected to asymmetric bending loads using nonlinear finite element methods. This study indicates that an increase in ship inclination can impact ultimate strength, particularly in sagging conditions. This research is relevant in the context of changes in the LPP length of Ro-Ro ships, which affect load distribution and structural response under bending loads [2].

Takami et al. developed a simulation method to predict the global and local hydroelastic response of ship structures. The proposed simulation method combines computational fluid dynamics (CFD) and finite element analysis (FEA). A comparison was made between CFD-FEA and other methods, such as tank testing, the linear/nonlinear strip method, and the 3D panel method, in terms of performance. The study identified that the proposed simulation model closely matched experimental results. However, it was noted that the simulation results showed reduced accuracy for the long wave range [3].

Xu et al. investigated the ultimate strength of an inland catamaran vessel under vertical bending moments. finite element method they used provided accurate results, [4].

The evaluation of the ultimate strength of ship hull girders has long been a fundamental aspect of naval architecture. Traditionally, this has been assessed through static monotonic loading methods, as introduced by

<sup>1</sup> Imam Pujo Mulyatno, Department of Naval Architecture, Diponegoro University, Semarang, 50275, Indonesia. E-mail: pujomulyatno2@gmail.com

<sup>2</sup> Ahmad Fauzan Zakky, Department of Naval Architecture, Diponegoro University, Semarang, 50275, Indonesia. E-mail: ahmadfauzanzakki@lecturer.undip.ac.id

<sup>3</sup> Kuku Prakoso Wicaksono, Department of Naval Architecture, Diponegoro University, Semarang, 50275, Indonesia. E-mail: kukuhrakoso@students.undip.ac.id

<sup>4</sup> Berlian Arswendo Adietya, Department of Naval Architecture, Diponegoro University, Semarang, 50275, Indonesia. E-mail: berlianarswendokapal@gmail.com

<sup>5</sup> Tuswan, Department of Naval Architecture Universitas Diponegoro, Semarang, 50275. E-mail: Tuswan@lecturer.undip.ac.id

Caldwell (1965). His approach involved subjecting the hull girder to extreme hogging or sagging bending moments in a one-time monotonic fashion. These moments typically correspond to conditions at least equivalent to half the wavelength of a critical wave, offering insight into the structure's ability to withstand extreme but isolated loading scenarios. This method formed the foundation for understanding the structural capacity of hull girders and their resistance to extreme bending during operations [5].

However, Fujita et al. (1984) highlighted a crucial limitation in the traditional monotonic approach. Ships operating in real-world conditions are subject to continuous cyclic bending moments induced by oscillating waves. These cyclic loads, comprising repetitive hogging and sagging effects, impose cumulative stresses on the hull girder, which differ fundamentally from the isolated static conditions assumed in earlier evaluations. Their findings indicated that cyclic loading could lead to progressive damage, a phenomenon not captured in monotonic tests, and thus warranted a more comprehensive approach to assessing ultimate strength. [6].

Subsequent studies expanded on this understanding, particularly the work of Liu and Soares (2020). Their detailed investigation revealed that hull girders under cyclic bending moments exhibit reduced ultimate strength compared to those subjected to monotonic loading. This reduction is attributed to the cumulative effects of cyclic stresses, such as progressive plastic deformation and fatigue damage, which gradually compromise structural integrity. These findings underscore the importance of incorporating cyclic loading scenarios into structural assessments, as they better represent the operational conditions encountered by ships [7].

Building on this perspective, Ji et al. (2021) further demonstrated that the ultimate strength of hull girders under cyclic loading tends to be significantly lower than under monotonic loading. Their research emphasized that the repetitive nature of cyclic stresses directly affects the structural behavior and durability of hull girders, offering critical insights for ship design aimed at enhancing operational safety over the vessel's lifespan. These findings reinforce the notion that cyclic loading effects must be accounted for in structural evaluations to prevent failures associated with long-term operational loads. [8].

The introduction of the shakedown concept by Jones (1975) marked a significant theoretical advancement in this field. Jones's research revealed that when the elastic-plastic behavior of hull girders is considered under cyclic loading, their longitudinal bending moment capacity is invariably reduced, or at best, equal to their monotonic ultimate strength. This principle provided a framework for understanding the degradation of structural performance due to cyclic effects, bridging the gap between theoretical analyses and practical considerations [9].

Taken together, these studies illustrate the critical need to transition from purely monotonic assessments to evaluations that incorporate cyclic loading effects. While

static methods offer foundational insights, they do not capture the progressive nature of damage caused by cyclic stresses. This shift is particularly relevant as operational conditions become more demanding, and the need for reliable, long-term structural performance becomes paramount.

Hu et al. analyzed the ultimate strength behavior of stiffened box girders subjected to extreme cyclic loading. Cracks were defined as transverse and through-thickness in the model configuration. An evaluation of the reinforced girder showed that a reduction in ultimate strength can occur under extreme cyclic loads. This approach may be applicable to reinforcing Ro-Ro ship structures to address increased loads due to hull length modifications [10].

Shi et al. investigated the effect of initial geometric imperfections on the ultimate strength dynamics. The research results indicated that geometric imperfections, such as shape irregularities, plate aspect ratios, and plate comparison, as well as the impact of velocity, significantly influence the dynamic behavior at the ultimate state [11]. In another study, the strength of the hull girder structure and Residual Strength in CSR (Common Structural Rules) Bulk Carriers and Oil Tankers was investigated to assess compliance with the new Residual Strength requirements under CSR-H. This implies that CSR-H ships have sufficient residual strength to withstand loads in calm and wave conditions even after sustaining damage [12].

Alfred Mohammed et al. conducted an analysis of the safety margin in the design of ultimate hull girder strength under combined vertical bending and torsional loads. The study results show that the vertical bending moment capacity of the hull girder decreases when torsional loading is included. The extreme values of the main components of global loads caused by waves, along with their combinations in irregular sea conditions, were predicted using the cross-spectral method, along with short- and long-term statistical formulations. Thus, the safety margin between the ultimate capacity and the expected maximum moment can be determined [13].

Myung-Su Yi et al. analyzed the causes of paint layer cracking that occurred in the cargo hold of a product transport vessel during tank testing and sea trials. They examined the structural behavior and mechanical loads with the aid of FEM to investigate the causes of these cracks, aiming to identify critical areas where ultimate strength occurs [14].

Shi and Wang studied a similar model for the ultimate strength of a ship's hull girder under combined bending and torsional loads. A similar model of the actual ship is derived based on thin-walled beam theory. The mathematical model is optimized to improve the design of structural dimensions. The consistency of the ultimate strength between the actual ship and this similar model is validated through nonlinear finite element methods under the influence of bending and torsional loads, allowing the similar model to be used in experiments to test the ultimate strength of the actual ship [15].

Bagas Ersa Pradana et al. analyzed the increase in ship dimensions and found that the bending moment and shear force increased significantly after modification. In the condition without vehicle loads (Light Weight Tonnage, LWT), the bending moment rose by 43.50%, and the shear force increased by 35.77%. Meanwhile, with vehicle loads, the bending moment increased by 41.38%, and the shear force rose by 43.24%. The average increase in the bending moment reached 42.44%. This increase enhances the ship's capacity, but the structural stability must still be considered [16].

Previous research analyzing the structural strength of ships using the FEM method on tanks, stiffeners, and the hull has not included studies on the midship compartment with added girders. This study will examine the effects of adding girders to the midship structure of the ship with high stiffness material, which is a new aspect that has not been thoroughly investigated in previous studies.

## II. METHOD

This research uses a Ro-Ro ship with a size of 2919 GT. The main dimensions of the ship are as follows: Overall Length: 93.768 m, Perpendicular Length: 81.605 m, Breadth: 24.5 m, Height: 4.8 m, Draft: 3.5 m, and Block Coefficient (CB): 0.74.

### A. Design Parameters for the Parallel Middle Body

The structure in the middle section of the ship (parallel middle body) is a crucial aspect of ship design, particularly in the field of naval engineering. Previous

research has shown that this area is the longest part of the ship with a constant cross-section [17]. The structural modeling in this section involves finite element analysis to ensure that the structure can withstand the loads applied, both from seawater pressure and the ship's cargo. Data regarding the ship's principal dimensions for the extension of the hull construction were taken from frames 39 to 46. Subsequently, changes to the construction length were made to align with this study.

This process includes the design of support beams and hull walls. Below are the specifications of the materials used: EH-36 Steel, modulus young: 200 GPa, Density: 7850 kg/m<sup>3</sup> shear modulus: 76.9 GPa, Yield Stregth: 355 MPa Poisson Rasio: 0.3.

### B. Concept of the Finite Element Method

The finite element method is a numerical approach used to solve linear elasticity problems in structures. These problems are addressed through the mathematical formulation of the appropriate differential equations, while also considering specific boundary conditions [18].

The introduction of the finite element method begins with the formulation of structural analysis using the displacement method [19].

### C. Modeling of the Parallel Middle Body

Development of a model based on the finite element method (FEM) for a Ro-Ro ship using commercial software, resulting in a multi-degree-of-freedom system..

In this study, three model variants were developed to

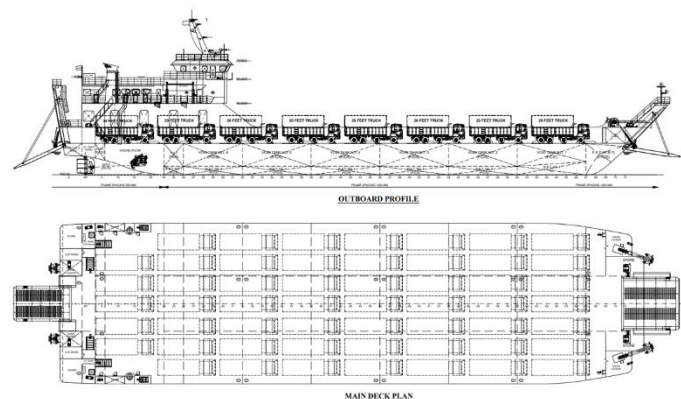


Figure 1 General Arrangement

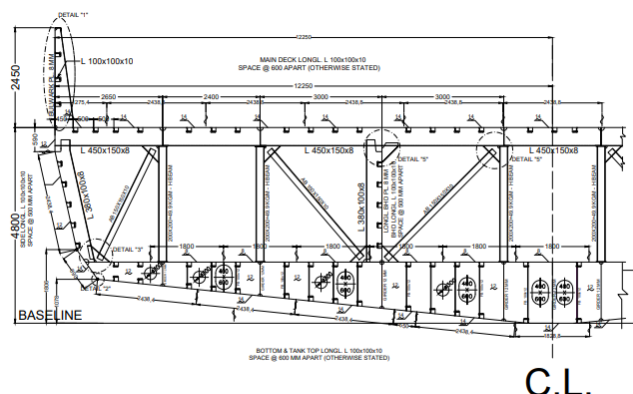


Figure 2. Frame Section

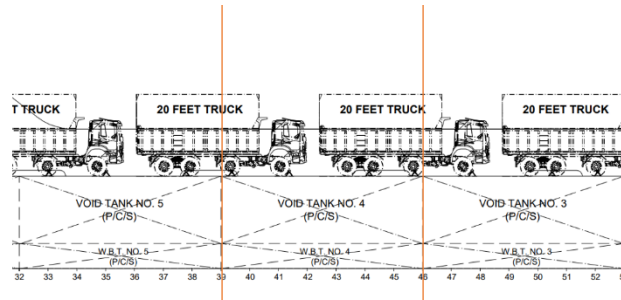


Figure 3. Selection of Frame (39–46)

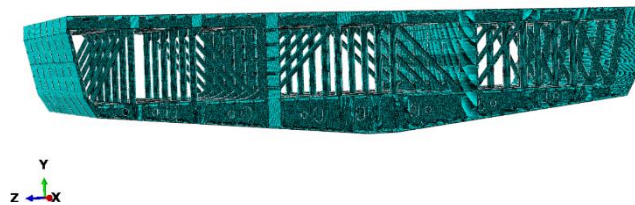


Figure 4. Geometry of Parallel Middle Body Using Finite Element Method.

compare the analysis results using the Finite Element Method (FEM), taking into account the variation in the length of the hull construction. The first model represents the ship structure before modifications, featuring 6 frames extending from F1 to F6, as shown in Figure 5. In the second model, after modifications, the number of frames increased to 8, extending from F1 to F8, as illustrated in Figure 6. Further modifications in the third model resulted in a total of 11 frames, maintaining the same range from F1 to F8, as demonstrated in Figure 7.

#### D. Meshing

The meshing process in the midsection of the ship (parallel middle body) using Finite Element Method (FEM) software is a crucial step in structural analysis [20]. In the midsection of the ship, which has a constant cross-sectional area, meshing must be done precisely to capture structural details such as the hull plates, stiffeners, and other supports. Good meshing ensures that the results of the FEM analysis can accurately represent the actual structural behavior of the midsection of the ship under various load conditions.

### III. RESULTS AND DISCUSSION

Based on the steps discussed above, this research will yield results regarding the impact of varying changes in the length of the longitudinal construction of the ship's hull due to changes in cargo load.

#### A. Boundary Conditions

Boundary conditions consist of rigid links at the ends of the model. These rigid links connect the nodes of the longitudinal construction at the ends of the model to independent points on the neutral axis along the centerline [21]. The boundary conditions that will be applied at the ends of the FEM model.

#### B. Load Definition

The vehicle load is generated from the vehicle cargo, which is distributed according to the general layout design of the vehicle on the car deck, in accordance with the field conditions, by transporting vehicles.

In Model 1 of the car deck, the weight of the vehicles (20 ft trucks) amounts to 7 units,

$$W = m \times g \quad (1)$$

$$W = 20 \text{ ton} \times 9,81 \text{ m/s}^2$$

$$= 196133 \text{ N}$$

load per unit area of the vehicle wheel,

$$P = \frac{W}{A} \quad (2)$$

$$P_{\text{Truk}} = \frac{196133 \text{ N}}{0,532 \text{ m}^2}$$

$$= 368573,68 \text{ N/m}^2$$

The vehicle weight on the cardeck Model 2 includes a total of 7 units of 40 ft trucks,

$$W = 38 \text{ ton} \times 9,81 \text{ m/s}^2$$

$$= 372652,7 \text{ N}$$

load per unit area of the vehicle wheel,

$$P_{\text{Truk}} = \frac{372652,7 \text{ N}}{0,684 \text{ m}^2}$$

$$= 544786,7 \text{ N/m}^2$$

The vehicle weight on the Model 3 car deck, with a mixture of vehicle weights (20 ft truck) totaling 7 units and vehicle weights (40 ft truck) totaling 7 units.

Hydrostatic pressure experienced by the ship's hull is due to the pressure exerted by seawater. This pressure is calculated based on the fundamental equation of hydrostatic pressure, which is directly influenced by the density of seawater ( $\rho$ ), gravitational acceleration ( $g$ ), and the depth or height of the ship's draft ( $h$ ) [22]. This phenomenon is one of the critical factors in ship structure design, as unbalanced pressure can lead to structural deformation.

$$P_h = \rho \times g \times h \quad (3)$$

$$P_h = 1025 \text{ kg/m}^3 \times 9,8 \text{ m/s}^2 \times 3,5 \text{ m}$$

$$= 35193,4 \text{ N/m}^2$$

and stress values obtained from the analysis using FEM Commercial software.

In the truck-loaded condition, the stress (von Mises) on the car deck is 9.582E+07 Pa or 95.82 MPa, with a maximum deformation of 1.8 mm on the car deck. The

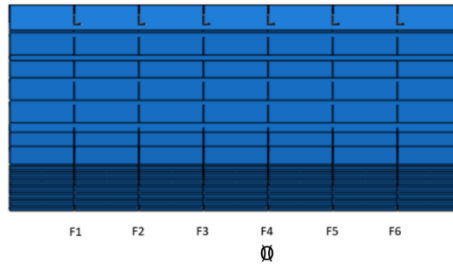


Figure 5. Model 1 (10.50 m)

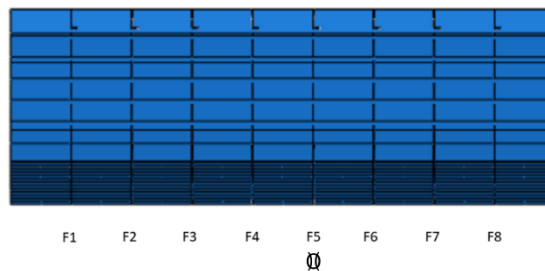


Figure 6. Model 2 (13.50 m)

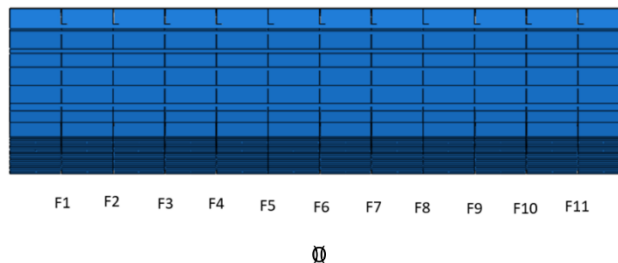


Figure 7. Model 3 (18.00 m)

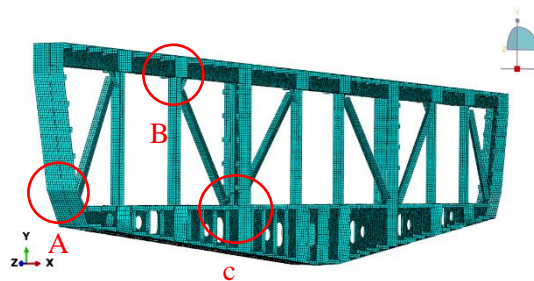


Figure 8. Meshing Transverse Web Frame 1

### C. Bending Moment

The calculations were performed using commercial software to obtain the moment values when the vessel is in calm water, sagging, and hogging conditions.

### D. Results of Analysis for Model 1 (L = 10.50 m)

Model Analysis 1 examines calm water conditions, including sagging and hogging, with the cardeck loaded with seven 20-foot trucks. The applied load consists of the ship's hydrostatic load. Below are the deflection values

maximum stress (von Mises) on the bracket is 1.45E+08 Pa or 145 MPa.

In the truck-loaded condition, the von Mises stress on the cardeck reaches 7.911E+08 Pa, or 79.1 MPa, on the longitudinal deck, with a maximum deformation of 1.835 mm. The maximum von Mises stress on the bracket is 1.777E+08 Pa, or 177.7 MPa.

In the loaded condition, the von Mises stress on the cardeck reaches 1.285E+08 Pa or 128.5 MPa on the longitudinal deck, with a maximum deformation of 2.9

mm. The maximum von Mises stress on the bracket is  $1.673E+08$  Pa or 167.3 MPa.

E. Results of Analysis for Model 2 (L = 13.50 m)

The analysis for Model 2 includes conditions of calm water, sagging, and hogging, with the cardeck loaded with seven 40-foot trucks. The applied loads

In the loaded condition, the von Mises stress on the cardeck is  $1.734E+08$  Pa or 173.4 MPa on the longitudinal deck, with a maximum deformation of 5.17 mm. The maximum von Mises stress on the bracket is  $2.016E+08$  Pa or 201.6 MPa.

F. Results of Analysis for Model 3 (L = 18.00 m)

Analysis Model 3 represents calm water conditions,

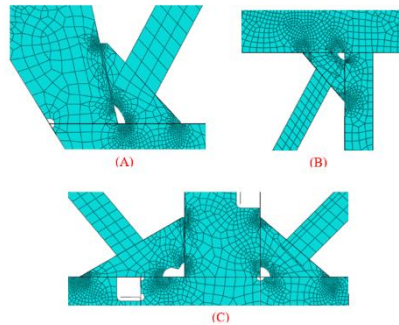


Figure 9. Finite Element Display of Brackets in the Transverse Web Frame

TABLE 1.  
BOUNDARY CONDITIONS

Location	Translation			Rotation		
	$\delta_x$	$\delta_y$	$\delta_z$	$\theta_x$	$\theta_y$	$\theta_z$
Rear End						
Independent point	-	fix	fix	-	-	-
Front End						
Independent point	fix	fix	fix	fix	-	-

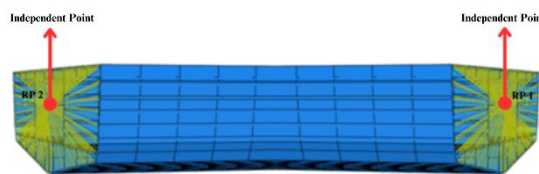


Figure 10. Boundary Conditions

include the ship's hydrostatic load. The following are the deflection and stress values obtained from the analysis using FEM Commercial software.

In the loaded condition, the von Mises stress on the cardeck is  $1.388E+08$  Pa or 138 MPa on the longitudinal deck, with a maximum deformation on the cardeck of 3.27 mm. The maximum von Mises stress on the bracket is  $1.741E+08$  Pa or 174.1 MPa.

In the truck-loaded condition, the Von Mises stress on the cardeck is  $1.186E+08$  Pa, or 118.6 MPa, on the longitudinal deck with a maximum deformation of 2.886 mm on the cardeck. The maximum Von Mises stress on the manhole reaches  $1.878E+08$  Pa, or 187.8 MPa.

sagging, and hogging, with the state being a cardeck loaded with a combination of 40-foot and 20-foot trucks. The loads considered include the hydrostatic load of the vessel. Below are the deflection and stress values obtained from the analysis using FEM Commercial software.

In the loaded condition, the maximum stress (von Mises) on the car deck is  $2.016 \times 10^8$  Pa or 201.6 MPa on the longitudinal deck, with a maximum deformation on the car deck of 6.2 mm.

In the loaded condition, the maximum stress (von Mises) on the car deck is  $1.986E+08$  Pa or 198.6 MPa on the longitudinal deck, with a maximum deformation of 4.52 mm on the car deck.

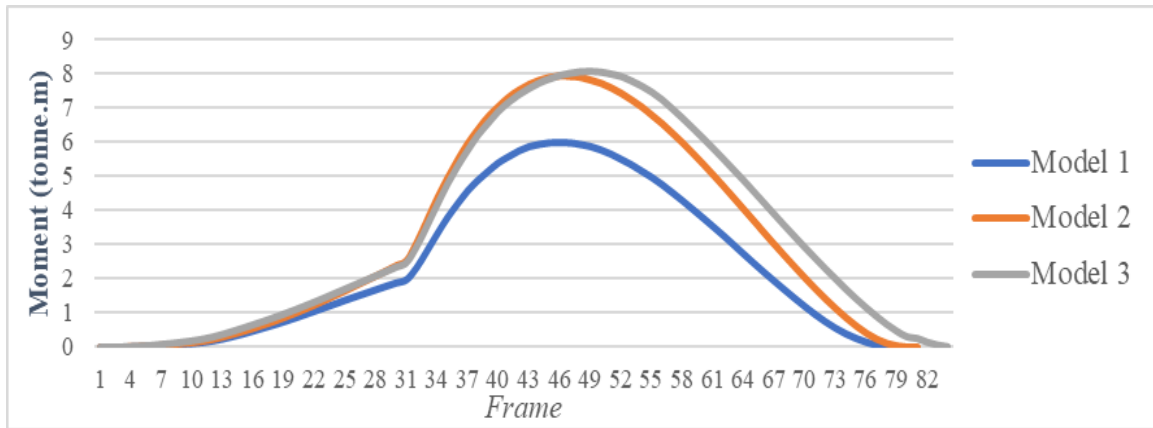


Figure 11. Graph of Moment Changes Under Still Water Conditions for Each Model

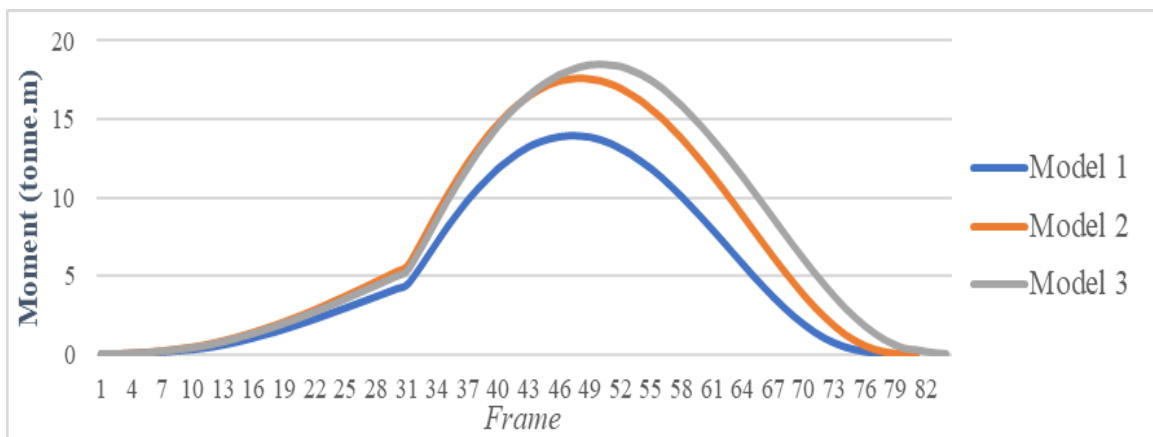


Figure 12. Graph of Moment Changes Under Hogging Conditions for Each Model

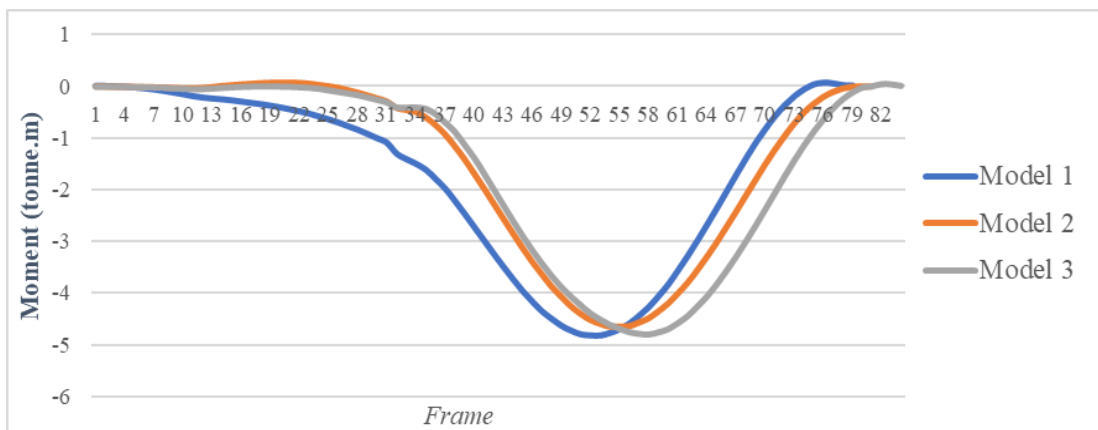


Figure 13. . Graph of Moment Changes Under Sagging Conditions for Each Model

In the loaded condition, the maximum stress (von Mises) on the cardeck is  $2.434E+08$  Pa or 243.4 MPa on the longitudinal deck, with a maximum deformation on the cardeck of 9.97 mm.

#### G. Calculation of Midship Section Modulus

The minimum midship section modulus value based on BKI Rules 2022 Vol. II Section 5 C.2.1 is used in the calculation of longitudinal strength [23[1]. Therefore, the value can be calculated using the formula:

$$W_{\min} = k \times c_0 \times L_2 \times B (C_B + 0.7) \times 10^{-6} \quad (4)$$

$$W > W_{\min} \quad (5)$$

Where  $W_{\min}$  is the minimum modulus value ( $m^3$ ),  $k$  is the material factor,  $c_0$  the wave coefficient,  $L$  is the length of the ship (m),  $B$  is the width of the ship (m), and  $C_B$  is the block coefficient of the ship. The modulus is calculated based on the Parallel Middle Body model. The calculated modulus values for the Ro-Ro ship are presented in Table 3.

#### H. Calculation of Deformation

TABLE 2.  
 MOMENT CALCULATION

Model	Conditions		
	Still Water	Sagging	Hogging
	Moment (kN.m)		
1	58732.03	-47307.3	136528.2
2	78060.93	-45493	172597
3	79296.57	-47022.9	181795.7

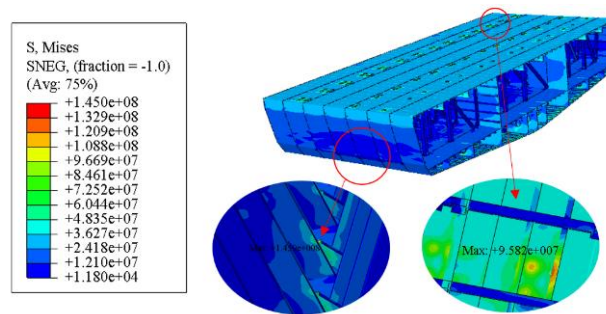


Figure 14. The stress on Model 1 Cardeck with Truck Load in Still Water Condition

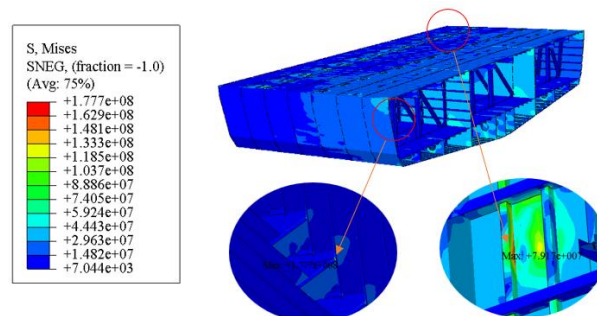


Figure 15. The stress on Model 1 Cardeck Loaded with Trucks in Sagging Condition

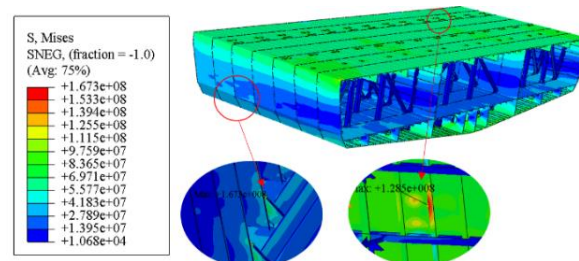


Figure 16. The stress on Model 1 Cardeck Loaded with Trucks in Hogging Condition

In this study, the verification of deformation results was conducted to compare the outcomes of deflection calculations from the commercial software with those from manual calculations. Based on the equations of manual calculations in engineering mechanics, the following equation can be used [24].

$$V_{max} = \frac{F \times L^3}{3 \times E \times I} \quad (5)$$

Description:

$V_{max}$  = Maximum Deflection

F = Force (N)

L = Length (m)

E = Modulus of Elasticity (N/m<sup>2</sup>)

I = Moment of Inertia (m<sup>4</sup>)

The manual calculation values for deformation in model creation have correction values of Model 1 (0.08%), Model 2 (1.52%), and Model 3 (0.42%). Therefore, the criteria for the results from both the commercial software and manual calculations are satisfied.



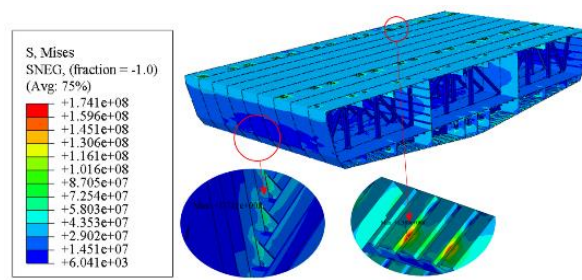


Figure 17. The stress on Model 2 Cardeck with Truck Load in Still Water Condition

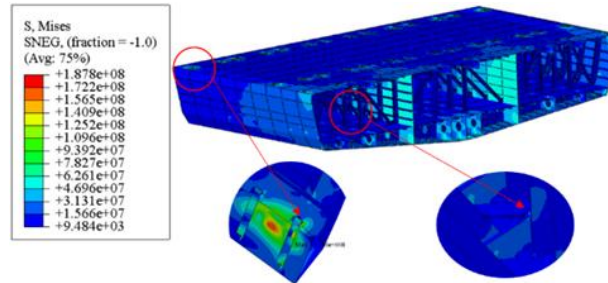


Figure 18. The stress on Model 2 Cardeck Loaded with Trucks in Sagging Condition

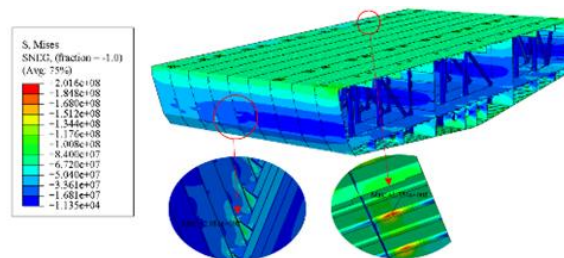


Figure 19. The stress on Model 2 Cardeck Loaded with Trucks in Hogging Condition

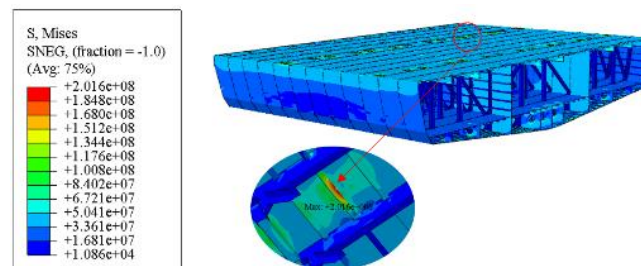


Figure 20. The stress on Model 3 Cardeck with Truck Load in Still Water Condition

### I. Summary of Structural Analysis Results

The results of the analysis from three conditions indicate that for the truck-loaded vessel, the maximum stress and deflection occur under hogging conditions. Among all the models analyzed, Model 3 exhibits the highest stress and deflection in every condition, indicating that this model has the greatest vulnerability to deformation and structural stress. Further data on the distribution of stress and deflection is presented in the following graph.

### J. Safety Factor

The safety factor is the ability of a material to withstand various external loads, including compressive

load and tensile load [25]. A structure is considered safe if the value  $S_f > 1$ .

The strength criteria for ship structures according to BKI regulations is 263 MPa, as stated in BKI Volume II Section 5 D.1.2. Table 6 presents a comparison of stress for each condition against the BKI strength criteria. The ship in conditions of calm water, sagging, and hogging meets the strength criteria set by BKI. Although in the hogging condition the maximum stress value approaches the allowable stress, which is 243.4 MPa, this value remains within the safe limits according to BKI criteria. Therefore, the ship's structure can be considered safe based on this analysis.

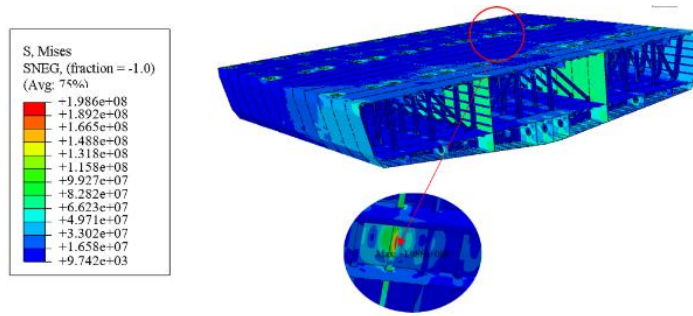


Figure 21. The stress on Model 3 Cardeck Loaded with Trucks in Sagging Condition

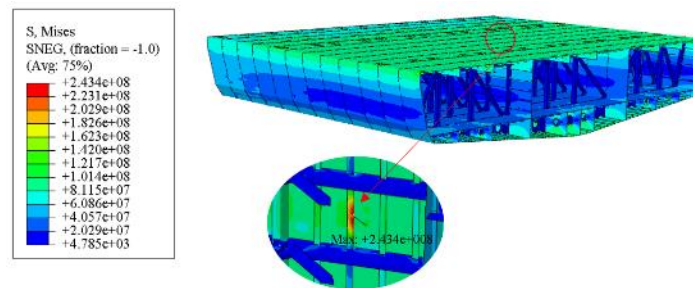


Figure 22. The stress on Model 3 Cardeck Loaded with Trucks in Hogging Condition

TABLE 3.  
SHIPS MODULUS CALCULATION

Model	Modulus	BKI Criteria	Description
W <sub>1</sub>	1,856	0,998599	Compliant
W <sub>2</sub>	1,856	1,445145	Compliant
W <sub>3</sub>	1,856	1,605613	Compliant

TABLE 4.  
VALUE OF L AND V<sub>max</sub>

Model	L	V <sub>max</sub>
1	10,5	1,26E-06
2	13,5	2,67E-06
3	18	6,33E-06

TABLE 5.  
VALUE OF L AND V<sub>max</sub>

Model	Manual Calculation (m)	Software Calculation (m)	Remarks
1	1,26E-06	1,27E-06	Compliant
2	2,67E-06	2,63E-06	Compliant
3	6,33E-06	6,31E-06	Compliant

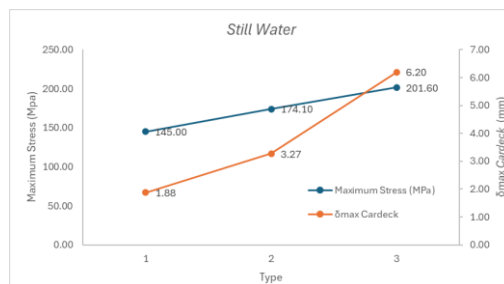


Figure 23. Maximum Stress Distribution and Maximum Deflection in Calm Water Conditions for Various Model

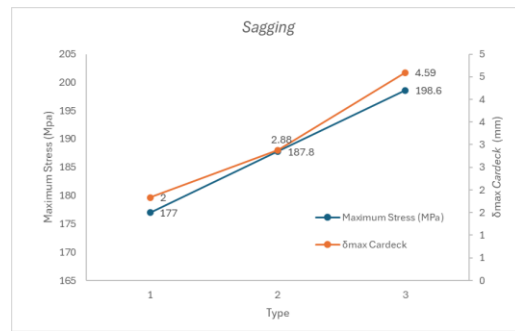


Figure 24. Maximum Stress Distribution and Maximum Deflection in Sagging Conditions for Various Calm Models

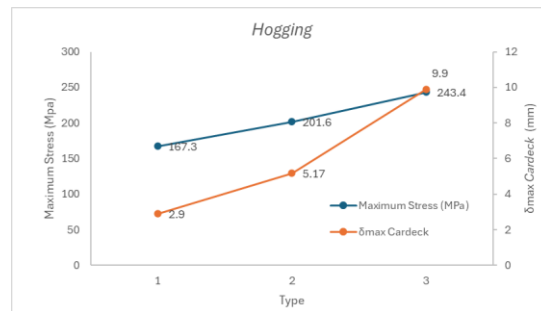


Figure 25. Maximum Stress Distribution and Maximum Deflection in Hogging Conditions for Various Models

TABLE 6.  
BKI STRENGTH CRITERIA FOR TRUCK-LOADED SHIPS IN STILL WATER, SAGGING, AND HOGGING

STILL WATER			
Model	Maximum Stress (MPa)	Allowable Stress (MPa)	Remarks
1	145	263	SAFE
2	174,1	263	SAFE
3	201,6	263	SAFE
Sagging			
1	177	263	SAFE
2	187,8	263	SAFE
3	198,6	263	SAFE
Hogging			
1	167,3	263	SAFE
2	201,6	263	SAFE
3	243,4	263	SAFE

#### IV. CONCLUSION

Based on the analysis of the structural strength of the hull on the Ro-Ro ship with a capacity of 2919 GT due to changes in hull construction length, the results indicate that all models remain safe under all three conditions: Calm Water, Sagging, and Hogging. This is because the maximum stress experienced is still below the safe limit of 263 MPa according to BKI strength criteria. However, under Hogging conditions, Model 3 shows stress levels approaching the safe limit, necessitating structural modifications to ensure the safety of the vessel.

#### REFERENCES

- [1] A. A. Mubarak, "Kekuatan Batas Lambung Kapal Dalam Menahan Momen Lentur Vertikal," *Jurnal Penelitian Enjiniring*, vol. 22, no. 1, pp. 56–61, 2019, doi: 10.25042/jpe.052018.10.
- [2] M. Tekgoz, Y. Garbatov, and C. Guedes Soares, "Strength assessment of an intact and damaged container ship subjected to asymmetrical bending loadings," *Marine Structures*, vol. 58, pp. 172–198, 2018, doi: 10.1016/J.MARSTRUC.2017.11.006.
- [3] T. Takami, S. Matsui, M. Oka, and K. Iijima, "A numerical simulation method for predicting global and local hydroelastic response of a ship based on CFD and FEA coupling," *Marine Structures*, vol. 59, pp. 368–386, 2018, doi: 10.1016/J.MARSTRUC.2018.02.009.
- [4] S. Xu, Z. Gu, W. Shen, Q. Lei, and W. Tang, "Experimental and numerical study on ultimate bearing capacity of pressure cabin for nuclear power ships," *Ocean Engineering*, vol. 198, p. 108123, 2020, doi: 10.1016/J.OCEANENG.2020.108123.
- [5] Caldwell, J.B., 1965. Ultimate longitudinal strength. *Transactions of RINA* 107, 411–430
- [6] Fujita, Y., Nomoto, T., Yuge, K., 1984. Behavior of deformation of structural members under compressive and tensile loads (18 report) —on the buckling of a column subjected to repeated loading. *J. Soc. Nav. Archit. Jpn.* 156, 346–354.
- [7] Liu, B., Soares, C.G., 2020. Ultimate strength assessment of ship hull structures subjected to cyclic bending moments. *Ocean Eng.* 215, 107685. Murray, J., 1953. *Structural Development of Tankers*. Europe

- [8] Ji, J., Liu, B., Chen, L., et al., 2021. Evaluation of cumulative collapse of a LNG carrier hull girder under dynamic cyclic bending moments. *Int. Conf. Offshore Mech. Arctic Eng.* 85123, V002T02A039. American Society of Mechanical Engineers.
- [9] Jones, N., 1975. On the shakedown limit of a ship's hull girder. *J. Ship Res.* 19 (2),118–121.)
- [10] K. Hu, P. Yang, and T. Xia, "Ultimate strength prediction of cracked panels under extreme cyclic loads considering crack propagation," *Ocean Engineering*, vol. 266, p. 112948, 2022, doi: 10.1016/J.OCEANENG.2022.112948.
- [11] G. jie Shi, D. yu Wang, B. Hu, and S. J. Cai, "Effect of initial geometric imperfections on dynamic ultimate strength of stiffened plate under axial compression for ship structures," *Ocean Engineering*, vol. 256, p. 111448, 2022, doi: 10.1016/J.OCEANENG.2022.111448.
- [12] G. J. Shi, D. W. Gao, and H. Zhou, "Analysis of Hull Girder Ultimate Strength and Residual Strength Based on IACS CSR-H," *Math Probl Eng.* vol. 2019, 2019, doi: 10.1155/2019/2098492.
- [13] E. A. Mohammed, S. Benson, S. Hirdaris, and R. S. Dow, "Design safety margin of a 10,000 TEH container ship through ultimate hull girder load combination analysis," *Marine Structures*, vol. 46, pp. 78–101, 2016.
- [14] M. S. Yi, K. C. Seo, and J. S. Park, "Study on the Root Causes and Prevention of Coating Cracks in the Cargo Hold of a Product Carrier," *Metals (Basel)*, vol. 12, no. 10, 2022, doi: 10.3390/met12101688.
- [15] G. J. Shi and D. Y. Wang, "Analysis of the similar model for ultimate strength subjected to combined action of bending and torsion of a container ship," *Journal of Shanghai Jiaotong University*, vol. 44, no. 6, pp. 782–786, 2010.
- [16] Bagas Ersya Pradana, Raden Dimas Endro Witjonarko, and Abdul Gafur, "Analisa Longitudinal Strength Kapal Terhadap Penambahan Panjang Kapal Pada Perairan Selat Lombok" *Proceedings Conference on Marine Engineering and its Application*, vol. 3, no. 1, pp. 45–52, 2020.
- [17] A. Biran, "Geometric Properties of Areas and Volumes," *Geometry for Naval Architects*, pp. 121–194, 2019, doi: 10.1016/B978-0-08-100328-2.00012-2.
- [18] R. L. T. O. C. Zienkiewicz, *The Finite Element Method: Its Basis and Fundamentals*, 5th ed., vol. 1. Butterworth-Heinemann, 2000.
- [19] A. F. Zakki, *Metode Elemen Hingga*. Lembaga Pengembangan dan Penjaminan Mutu Pendidikan Universitas Diponegoro, 2014.
- [20] Y.-Y. Yu, Y. Lin, and Z.-S. Ji, "New method for ship finite element method preprocessing based on a 3D parametric technique," *J Mar Sci Technol*, vol. 14, no. 3, pp. 398–407, 2009, doi: 10.1007/s00773-009-0058-1.
- [21] Iacs, "Common Structural Rules for Bulk Carriers and Oil Tankers," 2024.
- [22] V. E. Cardoso and S. Botello, "Parallel Meshing for Finite Element Analysis," in *High Performance Computer Applications*, I. Gitler and J. Klapp, Eds., Cham: Springer International Publishing, 2016, pp. 156–168.
- [23] P. Klasifikasi, K. Bagian, and K. Samudra, "Peraturan Lambung Edisi Konsolidasi 2022 Biro Klasifikasi Indonesia" 2022. [Online]. Available: [www.bki.co.id](http://www.bki.co.id)
- [24] James M. Gere And Stephen P. Timoshenko, *Mekanika Bahan*, Edisi ke-4. Ciracas, jakarta : Erlangga.
- [25] E.P. Popov, *Mechanics of Materials*, 2nd edition. New Jersey: Prentice-Hall Inc., 1994.